Orthogonality Properties of Characteristic Modes for Lossy Structures

Matti Kuosmanen, Pasi Ylä-Oijala, Jari Holopainen, and Ville Viikari, *Senior Member, IEEE*

***Abstract*— Orthogonality of the characteristic modes with respect to the weight operator of the generalized eigenvalue equation (GEE), and in the far-field, is investigated in the case of lossy conducting and dielectric objects. Linking the weight operator to radiated power is shown to provide orthogonal far fields in the lossless case. In the lossy case, both the orthogonality of the characteristic far fields and the weight operator orthogonality of the modal currents are satisfied with respect to the Hermitian inner products only for sufficiently symmetric geometries, such as a sphere. For irregular lossy shapes, independent of the symmetry of the formulation, the far-field orthogonality can be obtained only with respect to the symmetric (non-Hermitian) product. The weight operator orthogonality can be satisfied with (complex) symmetric formulations, but again only with respect to the symmetric product. Since the symmetric products are not related to any physical power quantity, the modes do not form a (radiated) power orthogonal set in the lossy case. Hence, for lossy structures, characteristic modes (CMs) do not satisfy their classical definition and they need to be redefined.**

***Index Terms*— Characteristic modes (CMs), conductor losses, dielectric losses, surface integral equation (SIE), volume integral equation (VIE).**

I. Introduction

CHARACTERISTIC modes (CMs) were originally introduced for lossless structures as modal functions that form a complete orthogonal set on the surface of a sphere with respect to radiated power [1]–[3]. These functions diagonalize the perturbation operator of a scattering problem and can be used to expand any field scattered or radiated by the object [2]. Harrington and Mautz [4] approached the same problem with an integral (impedance) operator relating the current on the surface of a perfect electric conductor (PEC) to the tangential electric field. They formulated a generalized eigenvalue equation (GEE) and showed that the solutions of the GEE diagonalize both the impedance and radiation operators.

In both perturbation and integral operator approaches, the key feature is the far-field orthogonality. As pointed out in [4], a symmetric weight operator can diagonalize the impedance operator, but only a weight operator related to the radiated power can provide orthogonal far fields. The same property was shown to be valid also with the volume integral equation (VIE)-based CM formulation for lossless dielectric non-magnetic bodies [5]. The common feature in these two formulations is that the GEE is expressed with real symmetric operators.

In the case of nonsymmetric operators, and for lossy objects, the situation is more complicated. Harrington *et al.* [5] and Chang and Harrington [6] tend to symmetrize the operators and express the GEE in terms of the Hermitian parts. This approach, applied for the Poggio–Miller–Chang–Harrington–Wu–Tsai (PMCHWT)-based surface integral equation (SIE) formulation [6], is found to produce spurious non-physical solutions [7]–[9].

In the lossy case, two alternative CM formulations have been proposed [5], [10]. The first one, producing complex eigensolutions, was argued to diagonalize both the scattering and impedance operators, thus providing also orthogonal far fields. The second one, giving real eigensolutions and diagonalizing the impedance operator only, was shown to have non-orthogonal far fields. The first approach is recently generalized for closed lossy impedance surfaces [11], for lossy dielectric and dielectric–magnetic [12], as well as for combined PEC and lossy dielectric objects [13].

In this article, we show that neither of the formulations for lossy metallic sheets introduced in [10] gives modes that simultaneously diagonalize both the impedance and radiation operators. The consequences of this result are investigated in the case of lossy dielectric and dielectric–magnetic objects following Harrington's first formulation type [5]. We use both the SIE-(PMCHWT) and VIE-based approaches, including symmetric and nonsymmetric formulations. To our knowledge, numerical solutions of the VIE approach for (lossy) dielectric–magnetic materials have not been considered before.

The orthogonality with respect to the radiated power operator is shown to be equivalent to the far-field orthogonality. In the lossless case, this implies that the weight operator related to the radiated power ensures orthogonal far fields. In the lossy case, the orthogonality properties of the CMs are found to depend also on the symmetry of the geometry. For sufficiently symmetric objects, such as a sphere (the results are not shown here, but this is obvious since the CMs match with the spherical modes), the CMs satisfy both the operator and the far-field orthogonalities. Numerical results of previous studies propose that this result holds also for a cube [9], [14].

For irregular nonsymmetric lossy dielectric geometries, none of the considered CM formulations satisfy the operator nor the far-field orthogonality with respect to the Hermitian inner product. However, in that case, the symmetric formulations satisfy orthogonality relations with respect to

Manuscript received 10 May 2021; revised 13 December 2021; accepted 14 January 2022. Date of publication 28 January 2022; date of current version 26 July 2022. *(Corresponding author: Matti Kuosmanen.)*

The authors are with the Department of Electronics and Nanoengineering, Aalto University, 02150 Espoo, Finland (e-mail: matti.s.kuosmanen@aalto.fi).

Color versions of one or more figures in this article are available at https://doi.org/10.1109/TAP.2022.3145441.

Digital Object Identifier 10.1109/TAP.2022.3145441

the symmetric product. This agrees with Harrington's result for the operator orthogonality [5] but disagrees with the far-field orthogonality. Although these symmetric orthogonality relations are not related to any physical (power) quantity, symmetric formulations are useful in the modal expansion, since the computation of the eigenvectors of the adjoint GEE [15] can be avoided.

II. Definition, Formulation, and Properties of Characteristic Modes

Let us consider time-harmonic electromagnetic fields with the time convention $e^{-i\omega t}$. We begin by reviewing the main features of the perturbation- and integral-operator-based CM formulations in the lossless case.

A. Perturbation Operator Formulation

Garbacz [2] introduced the mathematical basis for the CMs using scattering and perturbation operators of an arbitrarily shaped lossless object. The modes were obtained from an eigenvalue equation defined by

$$\mathcal{P}[\boldsymbol{f}_n] = \nu_n \boldsymbol{f}_n \tag{1}$$

where $\mathcal{P}$ is called the perturbation operator, ν_n is the eigenvalue, and $\boldsymbol{f}_n$ is the characteristic field pattern. The perturbation operator essentially describes how the object transforms converging fields to diverging fields in comparison with free space. Mathematically, it is related to the scattering operator $\mathcal{S}$ as follows:

$$\mathcal{P} = \frac{1}{2}(\mathcal{S} - \mathcal{I}) \tag{2}$$

where $\mathcal{I}$ is the identity operator.

Since the scattering problem maintains reciprocity, the corresponding scattering matrix is complex symmetric. In a lossless case, the scattering matrix is also unitary, and thus both the scattering and perturbation matrices are normal [2]. According to the spectral theorem [16], the eigenvectors of a normal matrix are orthogonal, that is, the scattering and perturbation matrices are unitarily similar to a diagonal matrix. In other words, the scattering matrix can be expressed as

$$S = U\, D\, U^H \tag{3}$$

where D is a diagonal matrix, matrix U is unitary, that is, $U^H U = I$, and $(\cdot)^H$ denotes Hermitian (complex conjugate) transpose.

The perturbation-operator-based CMs can be defined as a set of orthogonal far-field pattern functions that unitarily diagonalize both the scattering and perturbation operators.

B. Integral Operator Formulation

The integral operator formulation for the CMs starts with a linear integral equation of the scattering or radiation problem

$$\mathcal{L}[\boldsymbol{F}] = -\boldsymbol{G}^{\text{inc}}. \tag{4}$$

Here, $\mathcal{L}$ is a linear surface or volume integral operator, a generalized impedance operator,[1] $\boldsymbol{F}$ is a current density, and $\boldsymbol{G}^{\text{inc}}$ is a known incident field. In [4], a solution to (4) was found in the form of a GEE

$$\mathcal{L}[\boldsymbol{f}_n] = (1 - i\lambda_n)\mathcal{M}[\boldsymbol{f}_n] \tag{5}$$

where λ_n is an eigenvalue, $\boldsymbol{f}_n$ is an eigenvector, and $\mathcal{M}$ is a weight operator. Obviously, the choice of the operator $\mathcal{M}$ is crucial since it determines the properties of the eigenvalues and eigenvectors. The basic principle in this approach is to define $\mathcal{M}$ so that both the generalized impedance operator $\mathcal{L}$ and the radiation operator are simultaneously diagonalized.

The integral-operator-based CMs can now be defined as a set of weighted orthogonal currents, weighted with respect to the radiated power, which diagonalize both the radiation and the generalized impedance operators. A direct result from this definition is that the corresponding far fields are orthogonal and they also diagonalize the scattering operator.

The obvious difference between the perturbation-operator-based formulation and the integral-operator-based one is that the first one considers far-field eigenfunctions, while the second one deals with eigencurrents on the surface or volume of the object. As pointed out in [4], these two formulations lead to the same CMs with the same far-field properties. In the following, we consider only the integral operator approach.

C. Operator Orthogonality Relations

The way the CMs diagonalize the integral operators depends on the symmetry of the operators. Let us express (5) in the following form:

$$i(\mathcal{L} - \mathcal{M})[\boldsymbol{f}_n] = \lambda_n \mathcal{M}[\boldsymbol{f}_n]. \tag{6}$$

A special case is when the operators on the both sides of this equation are real and symmetric, that is, they satisfy

$$\langle \boldsymbol{g}, \mathcal{L}[\boldsymbol{f}] \rangle = \langle \mathcal{L}[\boldsymbol{g}], \boldsymbol{f} \rangle \tag{7}$$

with respect to the symmetric L^2 product

$$\langle \boldsymbol{u}, \boldsymbol{v} \rangle = \int_\Omega \boldsymbol{u} \cdot \boldsymbol{v}\, d\Omega. \tag{8}$$

Here, domain Ω is either a volume V or a surface S. If this is satisfied, and operator $\mathcal{M}$ is positive (or negative) definite, the characteristic eigencurrents $\boldsymbol{f}_n$ diagonalize operators $\mathcal{L}$ and $\mathcal{M}$ [16]. In other words, the following orthogonality relations hold [4], [5]:

$$\langle \boldsymbol{f}_m^*, \mathcal{L}[\boldsymbol{f}_n] \rangle = 0, \quad \langle \boldsymbol{f}_m^*, \mathcal{M}[\boldsymbol{f}_n] \rangle = 0, \quad \text{if } m \neq n. \tag{9}$$

In that case, the eigenvalues are also real and the eigenvectors are equiphase and can be chosen as real [16].

If one of the operators in (6) is complex symmetric, operators $\mathcal{L}$ and $\mathcal{M}$ are diagonalized with respect to the symmetric product, defined without the complex conjugate [5]

$$\langle \boldsymbol{f}_m, \mathcal{L}[\boldsymbol{f}_n] \rangle = 0, \quad \langle \boldsymbol{f}_m, \mathcal{M}[\boldsymbol{f}_n] \rangle = 0, \quad \text{if } m \neq n. \tag{10}$$

[1] Operator $\mathcal{L}$ can be interpreted as an impedance operator, that is, a mapping from the electric current to the electric field only in a few special cases. Generally, it involves magnetic currents and magnetic fields, as well.

In a general case of nonsymmetric operators, diagonalization is satisfied with respect to the eigenvectors $\boldsymbol{f}_n$ and the adjoint eigenvectors $\boldsymbol{g}_m$, according to [15]

$$\langle \boldsymbol{g}_m^*, \mathcal{L}[\boldsymbol{f}_n]\rangle = 0, \quad \langle \boldsymbol{g}_m^*, \mathcal{M}[\boldsymbol{f}_n]\rangle = 0, \quad \text{if } m \neq n. \tag{11}$$

Here, $\boldsymbol{g}_m$ is a solution of the adjoint GEE [15], [17]

$$\mathcal{L}^a[\boldsymbol{g}_m] = (1 + i\lambda_m^*)\mathcal{M}^a[\boldsymbol{g}_m] \tag{12}$$

and $\mathcal{L}^a$ and $\mathcal{M}^a$ are the adjoint operators of $\mathcal{L}$ and $\mathcal{M}$. For self-adjoint operators, $\mathcal{L}^a = \mathcal{L}$, $\mathcal{M}^a = \mathcal{M}$, and the eigenvectors $\boldsymbol{f}_n$ and $\boldsymbol{g}_n$ agree.

D. Power Orthogonality

The above-mentioned operator orthogonalities have a connection to the physical properties of the CMs. Let us next consider radiated P_n^{rad}, reactive P_n^{reac}, and dissipated P_n^{diss} power of an eigencurrent $\boldsymbol{f}_n$. The first two are defined with the complex Poynting vector as

$$P_n^{\text{rad}} = \frac{1}{2}\text{Re}\int_S (\boldsymbol{E}_n \times \boldsymbol{H}_n^*)\cdot \boldsymbol{n}\, dS \tag{13}$$

$$P_n^{\text{reac}} = -\frac{1}{2}\text{Im}\int_S (\boldsymbol{E}_n \times \boldsymbol{H}_n^*)\cdot \boldsymbol{n}\, dS + \omega W_n^{sto,in} \tag{14}$$

and with the corresponding eigenfields $\boldsymbol{E}_n$ and $\boldsymbol{H}_n$. Here, S is the surface of the object with unit normal vector $\boldsymbol{n}$, and $W_n^{sto,in}$ is related to the energy stored in the volume enclosed by S [4], [5]. The dissipative power P_n^{diss} due to dielectric losses is given by

$$P_n^{\text{diss}} = \frac{\omega}{2}\int_V \text{Im}(\varepsilon_1)\|\boldsymbol{E}_n\|^2\, dV \tag{15}$$

where V is the volume of the object and ε_1 is the dielectric permittivity of V. For lossy conductors

$$P_n^{\text{diss}} = \frac{1}{2}\int_S \text{Re}(Z_s)\|\boldsymbol{J}_n\|^2\, dS \tag{16}$$

where Z_s is the position-dependent surface impedance of the conductor and $\boldsymbol{J}_n$ is the electric surface current. In the following, we consider only structures with constant ε_1 and Z_s. The power quantities can also be expressed with operator inner products [18], [19]

$$P_n^{\text{rad}} = -\frac{1}{2}\text{Re}\langle \boldsymbol{f}_n^*, \mathcal{W}[\boldsymbol{f}_n]\rangle \tag{17}$$

$$P_n^{\text{diss}} = -\frac{1}{2}\text{Re}\langle \boldsymbol{f}_n^*, \mathcal{N}[\boldsymbol{f}_n]\rangle \tag{18}$$

$$P_n^{\text{reac}} = \frac{1}{2}\text{Im}\langle \boldsymbol{f}_n^*, (\mathcal{W} + \mathcal{N})[\boldsymbol{f}_n]\rangle. \tag{19}$$

Here, $\boldsymbol{f}_n$ is a modal surface or volume current, including both the electric and magnetic currents. Operator $\mathcal{W}$ contains the integral operators of the exterior region, defining the radiation properties and the reactive power stored in the near field. The material-dependent operators are included in $\mathcal{N}$. The exact forms of these operators will be given later.

E. Far-Field Orthogonality Relations

From (17) to (19), it is evident that only the Hermitian inner products (with complex conjugates) agree with physical power quantities. In the lossy case, however, two different types of orthogonality definitions of CMs are used [4], [5]. The first one is the Hermitian orthogonality, defined for the far fields as

$$\int_{S_\infty} \boldsymbol{E}_m^*(\boldsymbol{r})\cdot \boldsymbol{E}_n(\boldsymbol{r})\, dS = 0, \quad \text{if } m \neq n \tag{20}$$

where S_∞ is a spherical surface in the far-field region. Another type of orthogonality relation, called symmetric orthogonality, is defined without the complex conjugate

$$\int_{S_\infty} \boldsymbol{E}_m(\boldsymbol{r})\cdot \boldsymbol{E}_n(\boldsymbol{r})\, dS = 0, \quad \text{if } m \neq n. \tag{21}$$

F. Summary of the Properties of CMs

By combining the classical results [2]–[5] with [12], [15], the main properties of the CMs can be summarized in the lossless case as follows.

- P1 The eigenfields unitarily diagonalize the scattering operator.
- P2 The eigencurrents are not necessarily orthogonal, but the corresponding eigenfields are orthogonal in the far-field.
- P3 The eigenvalues are real and provide the ratio of reactive and radiated power.
- P4 The eigencurrents diagonalize the radiated and reactive power operators.
- P5 The eigencurrents diagonalize the generalized impedance operator and the weight operator. The exact form depends on the symmetry of the operators, as in Section II-B.

It is important to emphasize that these properties are valid for lossless structures only. In the following, we study them in the case of lossy structures.

III. CM Formulations for Lossy Metallic Sheets

To illustrate the role of the losses on the eigensolutions, we start with the electric field integral equation (EFIE) for an open metallic surface [10]

$$(\mathcal{Z} - Z_s\mathcal{I})[\boldsymbol{J}] = -\boldsymbol{E}^{\text{inc}} \tag{22}$$

with the EFIE impedance operator $\mathcal{Z} = \mathcal{R} + i\mathcal{X} = \eta_0\mathcal{T}_0$, (constant) surface impedance $Z_s = R_s + iX_s$, and incident field $\boldsymbol{E}^{\text{inc}}$. Here, η_0 is the wave impedance of vacuum and operator $\mathcal{T}_0$ is defined in Appendix B.

A. Radiated Power-Based Formulation

To connect the eigenvalues to radiated power, we choose $\mathcal{M} = \mathcal{R}$, and write the GEE as [18]

$$(\mathcal{Z} - Z_s\mathcal{I})[\boldsymbol{J}_n] = (1 - i\lambda_n)\mathcal{R}[\boldsymbol{J}_n]. \tag{23}$$

This formulation agrees with the first formulation of [10], and the eigenvalues have the following physical interpretation [18]:

$$\lambda_n = \frac{P_n^{\text{reac}}}{P_n^{\text{rad}}} + i\frac{P_n^{\text{diss}}}{P_n^{\text{rad}}} \tag{24}$$

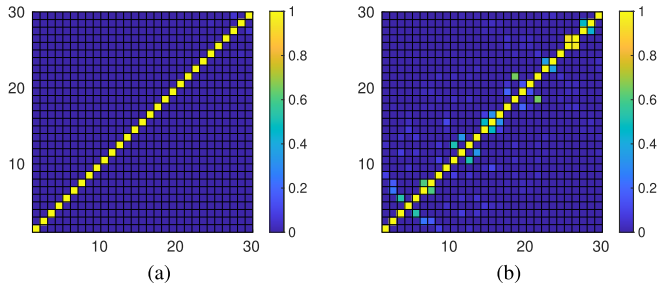

Fig. 1. Far-field correlation coefficient of the CMs (28) up to order 30 for a 1.0 m × 0.5 m rectangular plate at 300 MHz. (a) Lossless surface with $Z_s = 0.5i\eta_0$ and (b) lossy surface with $Z_s = 0.5\eta_0$. The axes correspond to mode indexes.

where the powers are defined as in (17)–(19) with $\mathcal{W} = \mathcal{Z}$ and $\mathcal{N} = -Z_s\mathcal{I}$. If the surface is a PEC, $Z_s = 0$, and (23) reduces to the well-known GEE with real and symmetric operators [4]

$$\mathcal{X}[\boldsymbol{J}_n] = -\lambda_n \mathcal{R}[\boldsymbol{J}_n]. \tag{25}$$

In that case, the obtained eigencurrents diagonalize both the impedance operator $\mathcal{Z}$ and the radiated power operator $\mathcal{R}$ and the modes are reactive and radiated power orthogonal. Consequently, the far fields of the modes are orthogonal, too.

Let us then consider a lossless surface with $Z_s = iX_s \neq 0$. In this case, the GEE reads

$$(\mathcal{X} - X_s\mathcal{I})[\boldsymbol{J}_n] = -\lambda_n \mathcal{R}[\boldsymbol{J}_n]. \tag{26}$$

Also here the operators on both sides of the GEE are real symmetric, and the same orthogonality properties hold as with PEC. However, a lossy surface with $Z_s = R_s > 0$, gives

$$(\mathcal{X} + iR_s\mathcal{I})[\boldsymbol{J}_n] = -\lambda_n \mathcal{R}[\boldsymbol{J}_n]. \tag{27}$$

The difference from the previous cases is that the operator on the left-hand side is not real symmetric, but it is complex symmetric. Therefore, the eigensolutions are complex and it is not obvious which orthogonality relations they satisfy.

Let us next illustrate this with a numerical example. In Fig. 1, we show the far-field correlation coefficient of modes m and n defined as

$$\rho_{nm} = \frac{\int_{S\infty} \boldsymbol{E}_n^* \cdot \boldsymbol{E}_m \, dS}{\sqrt{\int_{S\infty} \boldsymbol{E}_n^* \cdot \boldsymbol{E}_n \, dS}\sqrt{\int_{S\infty} \boldsymbol{E}_m^* \cdot \boldsymbol{E}_m \, dS}} \tag{28}$$

for a rectangular metallic plate at 300 MHz. We consider a lossless surface with $Z_s = \eta_0 0.5i$, and a lossy one with $Z_s = 0.5\eta_0$. The results in Fig. 1 suggest that the (Hermitian) far-field orthogonality is not necessarily satisfied in the lossy case as the correlation coefficient matrix includes non-zero off-diagonal elements.

B. Active Power-Based Formulation

In [5], another CM formulation for lossy structures was proposed. In this formulation, the weight operator is chosen as the real part of the operator $\mathcal{L}$, corresponding to active power, radiated plus dissipated, giving the following GEE:

$$(\mathcal{X} - X_s\mathcal{I})\big[\boldsymbol{J}_n^{(2)}\big] = -\lambda_n^{(2)}(\mathcal{R} - R_s\mathcal{I})\big[\boldsymbol{J}_n^{(2)}\big]. \tag{29}$$

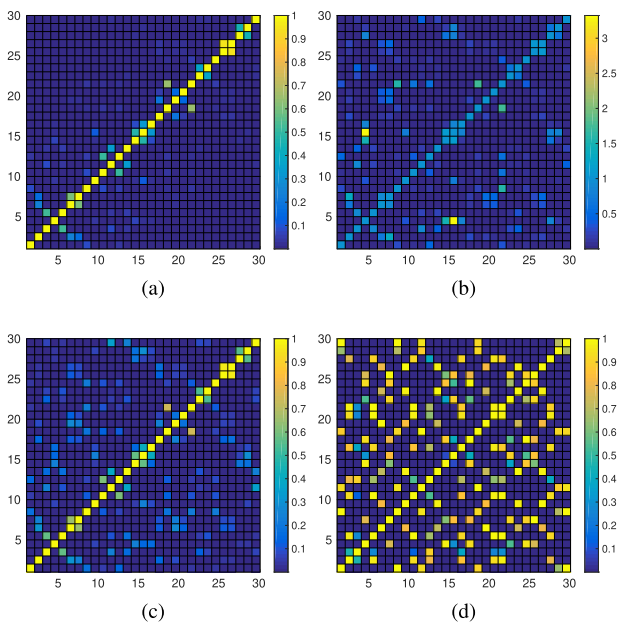

Fig. 2. Weighted inner products of the characteristic eigencurrents for a lossy 1.0 m × 0.5 m rectangular plate with $Z_s = 0.5\eta_0$ at 300 MHz, with respect to (a) radiated, (b) reactive, and (c) dissipated power operators for radiated power-based formulation (23). (d) Far-field correlation coefficient of the modal fields for active power-based formulation (29). The axes give the mode indexes.

Clearly, in the lossless case, $\mathrm{Re}(Z_s) = R_s = 0$, and this formulation agrees with (25). In the lossy case, however, the active power and radiated power formulations do not agree. The eigenvalues of (29) have the following interpretation [18]:

$$\lambda_n^{(2)} = \frac{P_n^{\mathrm{reac}}}{P_n^{\mathrm{rad}} + P_n^{\mathrm{diss}}}. \tag{30}$$

This formulation diagonalizes the impedance operator but does not provide orthogonal far fields in the lossy case [10].

To further illustrate the effect of losses, and the differences between the two formulations, Fig. 2 shows orthogonality of the CMs of the radiated power-based formulation with respect to the radiated $\mathcal{R}$, reactive $(\mathcal{X} - X_s\mathcal{I})$, and dissipated, $R_s\mathcal{I}$, power operators. In this figure, also the far-field orthogonality of the solutions of the active power-based formulation is shown. In Fig. 3, the real parts of the eigenvalues of the radiated and active power-based formulations are plotted as the losses, that is, $\mathrm{Re}(Z_s)$, are increased.

From these results, the following observations can be made.

1) The far-field orthogonality is identical with the radiated power orthogonality.
2) The non-orthogonality is stronger with respect to the reactive and dissipated power operators than with respect to the radiated power operator.
3) In the lossy case, the active power-based formulation (29) leads to much stronger non-orthogonality in the far fields than the radiated power-based one (23).
4) The eigenvalues of the formulation (29) tend to approach zero as losses are increased, while in (23), the losses contribute to the imaginary part only, providing separation of the radiated, reactive, and dissipated power.

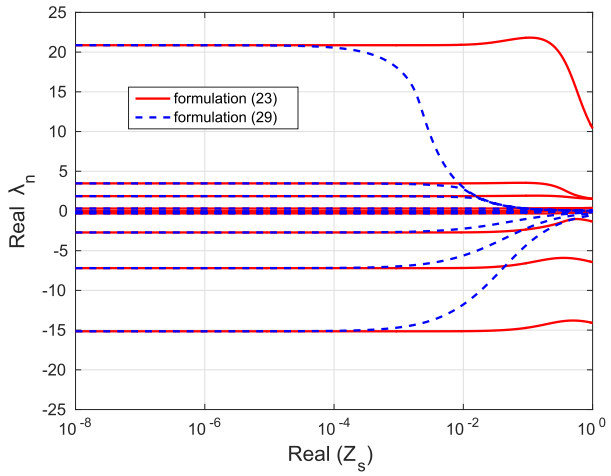

Fig. 3. Real parts of the eigenvalues of the radiated power formulation (23) and active power formulation (29) for a 1 m × 0.5 m lossy metallic sheet versus the real part of the surface impedance Z_s/η_0.

5) The active power-based formulation (29) diagonalizes the real and imaginary parts of the impedance operator, and thus the full impedance operator. As a consequence, the modes are orthogonal with respect to both active and reactive power.

IV. CM Formulations and Orthogonality Properties for Lossy Dielectric–Magnetic Objects

From the results of Section III, we may conclude that only the first formulation type, based on the radiated power operator, provides separation of the powers for lossy structures. In this section, we consider the properties of similar formulations in the case of lossy dielectric and dielectric-magnetic bodies. We investigate the effect of losses on the orthogonality properties of the solutions of two alternative CM formulations. The first one is based on VIE formulation [5] and the second one on the PMCHWT SIE formulation [9], [12]. Both symmetric and nonsymmetric forms are considered.

The electromagnetic material properties of the background and a homogeneous and isotropic object are characterized by constant parameters ε_0, μ_0 (vacuum) and ε_1, μ_1, respectively. The object can be lossy with complex permittivity defined as

$$\varepsilon_1 = \varepsilon_1' + i\sigma_1/\omega = \varepsilon_0\left(\varepsilon_r' + i\varepsilon_r''\right). \tag{31}$$

Here, σ_1 is the conductivity of the material.

A. Volume Formulation for Dielectric-Magnetic Bodies

With the volume integral operators (VIOs) given in Appendix A, we define two other VIOs. The first one depends only on the shape of the body [5], [18]

$$\mathcal{W}_V = \begin{bmatrix} \dfrac{i}{\omega\varepsilon_0}\mathcal{V} & -\mathcal{U} \\ \mathcal{U} & \dfrac{i}{\omega\mu_0}\mathcal{V} \end{bmatrix} = \begin{bmatrix} \mathcal{V}_\epsilon & -\mathcal{U} \\ \mathcal{U} & \mathcal{V}_\mu \end{bmatrix} \tag{32}$$

while the second depends on the material parameters [5], [18]

$$\mathcal{N}_V = \begin{bmatrix} \dfrac{1}{i\omega\varepsilon_0}\dfrac{1}{\epsilon_r - 1}\mathcal{I} & 0 \\ 0 & \dfrac{1}{i\omega\mu_0}\dfrac{1}{\mu_r - 1}\mathcal{I} \end{bmatrix} = \begin{bmatrix} \mathcal{I}_\epsilon & 0 \\ 0 & \mathcal{I}_\mu \end{bmatrix}. \tag{33}$$

The (nonsymmetric) VIE for a dielectric–magnetic object can now be expressed compactly with these operators as follows:

$$(\mathcal{W}_V + \mathcal{N}_V)[\boldsymbol{F}_V] = -\boldsymbol{G}^{\text{inc}} \tag{34}$$

where $\boldsymbol{G}^{\text{inc}} = [\boldsymbol{E}^{\text{inc}}, \boldsymbol{H}^{\text{inc}}]^T$ is the incident electromagnetic field and $\boldsymbol{F}_V = [\boldsymbol{J}_V, \boldsymbol{M}_V]^T$. The complex power balance of the body can be expressed with these operators as in (17)–(19). The radiated power can also be expressed as

$$\text{Re}\left\langle \boldsymbol{F}_V^*, \mathcal{W}_V[\boldsymbol{F}_V]\right\rangle = \begin{bmatrix} \boldsymbol{J}_V \\ \boldsymbol{M}_V \end{bmatrix}^{\text{H}} \underbrace{\begin{bmatrix} \text{Re}(\mathcal{V}_\epsilon) & -i\text{Im}(\mathcal{U}) \\ i\text{Im}(\mathcal{U}) & \text{Re}(\mathcal{V}_\mu) \end{bmatrix}}_{\mathcal{M}_V} \begin{bmatrix} \boldsymbol{J}_V \\ \boldsymbol{M}_V \end{bmatrix}. \tag{35}$$

By selecting $\mathcal{M}_V$ as the weight operator, the GEE reads

$$(\mathcal{W}_V + \mathcal{N}_V)[\boldsymbol{F}_n] = (1 - i\lambda_n)\mathcal{M}_V[\boldsymbol{F}_n]. \tag{36}$$

This is the generalization of the first VIE formulation of [5], resulting in the formulation for lossy dielectric–magnetic objects.

If the body is non-magnetic, the operators of (36) become

$$\mathcal{W}_V^D = \mathcal{V}_\epsilon, \quad \mathcal{N}_V^D = \mathcal{I}_\epsilon, \quad \mathcal{M}_V^D = \text{Re}(\mathcal{V}_\epsilon). \tag{37}$$

As a result, the GEE reads [5]

$$(\text{Im}(\mathcal{V}_\epsilon) - \mathcal{I}_\epsilon)[\boldsymbol{J}_n] = -\lambda_n \text{Re}(\mathcal{V}_\epsilon)[\boldsymbol{J}_n] \tag{38}$$

which is the well-known VIE-based CM formulation for dielectric bodies [5].

B. PMCHWT-Based Surface Formulation

Next, we present the required operators and GEEs with the PMCHWT-based SIE formulation. With the SIOs defined in Appendix B, PMCHWT equations are given by

$$\begin{bmatrix} \eta_0\mathcal{T}_0 + \eta_1\mathcal{T}_1 & -\mathcal{K}_0^+ - \mathcal{K}_1^- \\ \mathcal{K}_0^+ + \mathcal{K}_1^- & \dfrac{1}{\eta_0}\mathcal{T}_0 + \dfrac{1}{\eta_1}\mathcal{T}_1 \end{bmatrix} \begin{bmatrix} \boldsymbol{J}_S \\ \boldsymbol{M}_S \end{bmatrix} = -\begin{bmatrix} \gamma_t \boldsymbol{E}^{\text{inc}} \\ \gamma_t \boldsymbol{H}^{\text{inc}} \end{bmatrix} \tag{39}$$

with the wave impedance $\eta_j = \sqrt{\mu_j/\varepsilon_j}$, $j = \{0, 1\}$. By arranging the operators of the background with index 0 in $\mathcal{W}_P$ and the operators with index 1 in $\mathcal{N}_P$, (39) can be expressed as [9]

$$(\mathcal{W}_P + \mathcal{N}_P)[\boldsymbol{F}_S] = -\gamma_t \boldsymbol{G}^{\text{inc}} \tag{40}$$

with $\boldsymbol{F}_S = [\boldsymbol{J}_S, \boldsymbol{M}_S]^T$. Using these notations, the complex power balance can be expressed as in (17)–(19).

Following the formulation proposed in [9] and [12], the weight operator is chosen as

$$\mathcal{M}_P = \begin{bmatrix} \text{Re}(\eta_0\mathcal{T}_0) & -i\text{Im}(\mathcal{K}_0) \\ i\text{Im}(\mathcal{K}_0) & \text{Re}(1/\eta_0\mathcal{T}_0) \end{bmatrix}. \tag{41}$$

Here, $\mathcal{K}_j$ is the same as in (56) but without the residual term. This choice of the weight operator again relates the equivalent surface current to the radiated power, and the GEE reads

$$(\mathcal{W}_P + \mathcal{N}_P)[\boldsymbol{F}_n] = (1 - i\lambda_n)\mathcal{M}_P[\boldsymbol{F}_n]. \tag{42}$$

C. Symmetric Formulations

In [5], a symmetric form of the VIE formulation was proposed. In this formulation, the operators read

$$\mathcal{W}_V^S = \begin{bmatrix} \mathcal{V}_\epsilon & i\mathcal{U} \\ i\mathcal{U} & \mathcal{V}_\mu \end{bmatrix}, \quad \mathcal{N}_V^S = \begin{bmatrix} \mathcal{I}_\epsilon & 0 \\ 0 & \mathcal{I}_\mu \end{bmatrix}. \tag{43}$$

Clearly, the second operator, which depends on the material properties of the body, is unchanged. For the PMCHWT equations, the same symmetrization process gives operators [6]

$$\mathcal{W}_P^S = \begin{bmatrix} \eta_0\mathcal{T}_0 & i\mathcal{K}_0^+ \\ i\mathcal{K}_0^+ & \dfrac{1}{\eta_0}\mathcal{T}_0 \end{bmatrix}, \quad \mathcal{N}_P^S = \begin{bmatrix} \eta_1\mathcal{T}_1 & i\mathcal{K}_1^- \\ i\mathcal{K}_1^- & \dfrac{1}{\eta_1}\mathcal{T}_1 \end{bmatrix}. \tag{44}$$

Here, both operators are modified. In order to have the same eigensolutions as with the nonsymmetric PMCHWT-based formulation, the weight operator for the symmetric sPMCHWT formulation should be defined as [9] and [12]

$$\mathcal{M}_P^S = \begin{bmatrix} \mathrm{Re}(\eta_0\mathcal{T}_0) & -\mathrm{Im}(\mathcal{K}_0) \\ -\mathrm{Im}(\mathcal{K}_0) & \mathrm{Re}(1/\eta_0\mathcal{T}_0) \end{bmatrix}. \tag{45}$$

Analogously, for the symmetric VIE (sVIE), we define

$$\mathcal{M}_V^S = \begin{bmatrix} \mathrm{Re}(\mathcal{V}_\epsilon) & -\mathrm{Im}(\mathcal{U}) \\ -\mathrm{Im}(\mathcal{U}) & \mathrm{Re}(\mathcal{V}_\mu) \end{bmatrix}. \tag{46}$$

In the lossless case, operator $\mathcal{N}_V^S$ is purely imaginary, and thus

$$\mathrm{Re}\big(\mathcal{W}_V^S + \mathcal{N}_V^S\big) = \mathrm{Re}\big(\mathcal{W}_V^S\big) = \mathcal{M}_V^S. \tag{47}$$

The GEE for the sVIE can now be expressed as

$$\mathrm{Im}\big(\mathcal{W}_V^S + \mathcal{N}_V^S\big)\big[\boldsymbol{F}_n^S\big] = -\lambda_n \mathrm{Re}\big(\mathcal{W}_V^S + \mathcal{N}_V^S\big)\big[\boldsymbol{F}_n^S\big] \tag{48}$$

with $\boldsymbol{F}_n^S = [\boldsymbol{J}_n, i\boldsymbol{M}_n]^T$. In other words, in the lossless case, the GEE of the sVIE can be expressed in terms of its real and imaginary parts, and the operators are real and symmetric. In the lossy case, operator $\mathcal{N}_V^S$ is complex, and the operator on the left-hand side of the GEE becomes complex symmetric, while the weight operator is still real symmetric.

For sPMCHWT formulation, the situation is different. In both lossless and lossy cases, the material-dependent operator $\mathcal{N}_P^S$ is complex. This implies that in all cases, the operator on the left-hand side of the GEE is complex symmetric, while the weight operator is real symmetric [12]. In addition, since

$$\mathrm{Re}\big(\mathcal{W}_P^S + \mathcal{N}_P^S\big) \neq \mathrm{Re}\big(\mathcal{W}_P^S\big) = \mathcal{M}_P^S \tag{49}$$

the GEE for the sPMCHWT cannot be expressed in terms of its real and imaginary parts, as proposed in [6].

D. Verification of the VIE and SIE CM Formulations

To verify the solutions of VIE and SIE CM formulations, two test objects are used, as specified in Table I.

Fig. 4 shows the real and imaginary parts of the eigenvalues of ten lowest order modes computed with the nonsymmetric and symmetric VIE formulations and nonsymmetric PMCHWT formulation. The results are given as functions of the imaginary part of ε_r of the objects at 3 GHz.

The results in Fig. 4 suggest that the VIE- and PMCHWT-based approaches give eigenvalues with essentially the same behavior in both cases of lossy dielectric and lossy dielectric–magnetic bodies. Some differences in the numerical values can be observed due to numerical approximations. In addition, the eigenvalues have the same physical interpretation as in (24).

TABLE I

PROPERTIES OF THE TEST OBJECTS. D-BRICK REFERS TO DIELECTRIC MATERIAL AND DM-BRICK TO DIELECTRIC–MAGNETIC MATERIAL

Test brick	Size (mm×mm×mm)	ε_r'	ε_r''	μ_r
D-brick	25.40 × 19.05 × 12.70	9.1	0.01…100	1
DM-brick	25.40 × 19.05 × 12.70	3.5	0.01…100	2.6

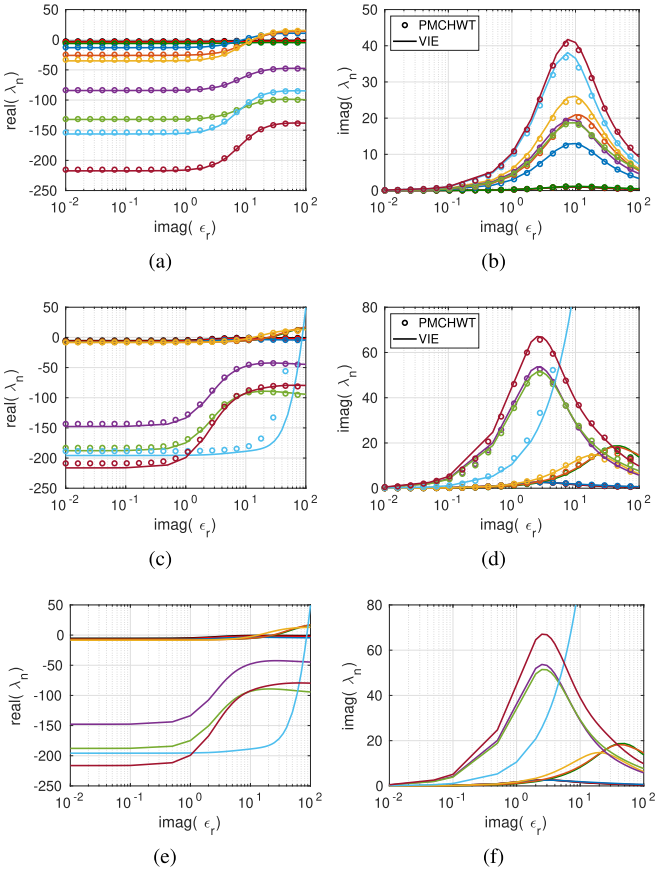

Fig. 4. Eigenvalues versus ε_r'' at 3 GHz: (a) real part for D-brick (b) imaginary part for D-brick, (c) real part for DM-brick, (d) imaginary part for DM-brick. (e) Real and (f) imaginary parts with sVIE for DM-brick.

E. Inner Product and Far-Field Orthogonalities

Next, we study the orthogonality properties of the modes. In Fig. 5, we show the weighted inner products and far-field correlation coefficients of the modes computed with the VIE and PMCHWT formulations in the case of the D-brick with $\varepsilon_r = 9.1 + 10i$. Visually, the results are nearly identical.

Next, we illustrate that the modes of the VIE and PMCHWT formulations satisfy the symmetric far-field orthogonalities, that is, as (28) is defined without the complex conjugate. These results are shown in Fig. 6. It is important to note that the CMs of the nonsymmetric formulations do not satisfy symmetric operator orthogonality relations (10).

F. Diagonal Dominance of the Matrices

Another point of view on the orthogonality of the modes can be obtained by studying the diagonal dominance of the

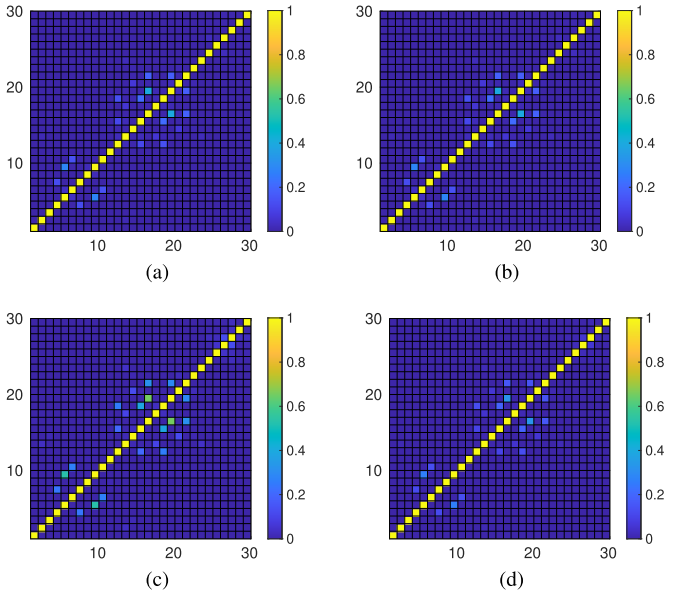

Fig. 5. Hermitian weighted inner products (9) of the characteristic eigencurrents: (a) VIE and (c) PMCHWT. Hermitian far-field correlation coefficient (28) of the characteristic fields: (b) VIE and (d) PMCHWT. D-brick with $\varepsilon_r = 9.1 + 10i$ at 3 GHz.

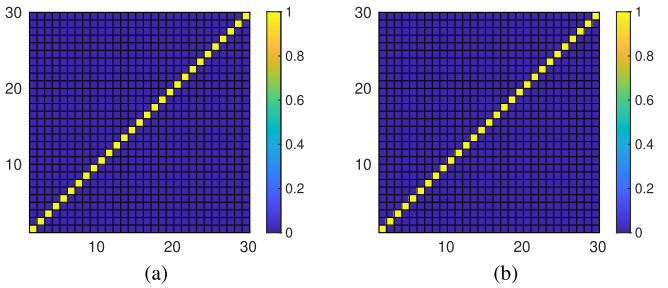

Fig. 6. Symmetric far-field correlation coefficient: (a) VIE and (b) PMCHWT formulation. D-brick with $\varepsilon_r = 9.1 + 10i$ at 3 GHz.

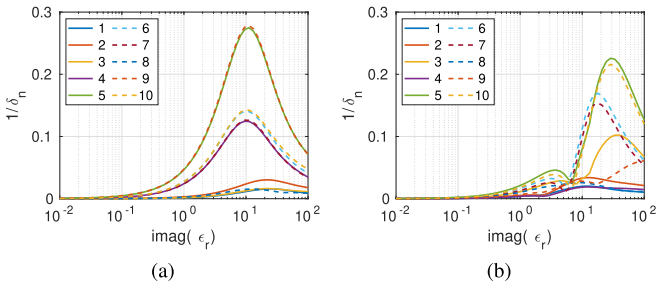

Fig. 7. Inverse of $\delta_n, n = 1, \ldots, 10$, as a function of ε_r'' with PMCHWT formulation at 3 GHz. (a) D-brick and (b) DM-brick.

inner product matrix

$$\delta_n = \frac{|A_{nn}|}{\sum_m |A_{mn}|}, \quad m \neq n \tag{50}$$

where $\boldsymbol{A}$ is defined with $\mathcal{M}$, the weight operator of the GEE

$$A_{mn} = \left\langle \boldsymbol{F}_m^*, \mathcal{M}[\boldsymbol{F}_n] \right\rangle. \tag{51}$$

Fig. 7 shows the inverse of δ_n for the D- and DM-bricks computed with the (nonsymmetric) PMCHWT formulation.

By comparing the results of Figs. 4(b) and 7(a), a clear correlation between the diagonal dominance of the inner product matrix and the imaginary part of the eigenvalues of the modes can be observed. In the case of a dielectric–magnetic brick, the correlation is not as obvious. In addition, a correlation between Figs. 4(b) and 5 can be observed. For example, Fig. 5 shows that modes 5 and 9 correlate only with each other. Thus, their diagonal dominance factors are identical.

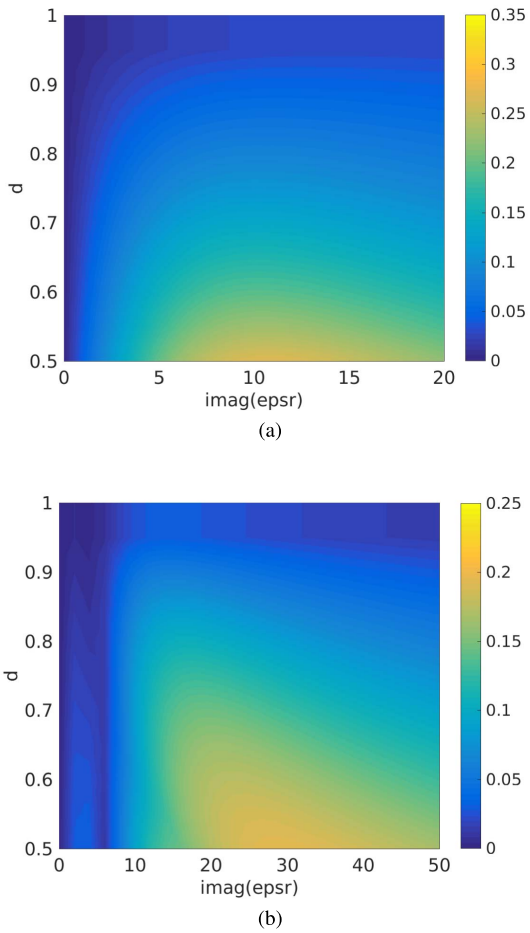

Fig. 8. Maximum of $1/\delta_n, n = 1, \ldots, 10$, versus ε_r'' and geometry parameter d at 3 GHz. $d = 1$ is a cube with edge length 25.40 mm, $d = 0.5$ is a 25.40 mm$\times$ 19.05 mm $\times$ 12.70 mm brick. (a) D-brick and (b) DM-brick. PMCHWT formulation.

In the last example, we vary both the geometry and the imaginary part of the permittivity. Fig. 8 shows the maximum of the inverse of the diagonal dominance for the ten first modes as a function of the imaginary part of the relative permittivity ε_r'' and symmetry parameter d. We observe that the diagonal dominance depends also on the geometry. For a cube, as $d = 1$, the inner product matrix is more diagonally dominant than for a brick, agreeing with the results presented in [9] and [14].

V. Discussion

The integral operator-based theory of CMs with real symmetric operators is well established in the case of PEC-only structures [4]. The corresponding theory and the properties of the CMs for dielectric, and, in particular, for lossy materials have been found to be much complicated and less known. For these reasons, to date, the CMs have been mainly applied for lossless conducting structures [20]. Since the losses have not

attained much attention before, the definition of CMs in the lossy case has been uncertain.

Garbacz [1], Garbacz [2], and Garbacz and Turpin [3] did not consider losses at all, and Harrington *et al.* [5] and Harrington and Mautz [10] gave only a rather brief presentation of the theory for lossy dielectric objects without further analysis. In [5], two alternative formulations for lossy penetrable objects were proposed. However, even though those formulations look mathematically solid, they included serious shortcomings. The first, the radiated power-based one, lacks both the power and far-field orthogonality property since the GEE cannot be expressed solely with real symmetric or Hermitian operators. The active power-based one is able to provide orthogonality with respect to the reactive and active power and thus also diagonalizes the impedance operator, but does not give orthogonal far fields.

With any formulation, we always end up with the same problem: the modes cannot be orthogonal with respect to the three power quantities, radiated, dissipated, and reactive power, at the same time. Therefore, the classical definition of CMs, which requires orthogonal far fields and orthogonal complex power balance, cannot be satisfied. On the other hand, always two of these three power quantities can be orthogonalized. These formulations, where one of the power-related operators is dropped out, produce solutions that cannot be considered as CMs, but that could be useful in various situations [21].

VI. Conclusion

Orthogonality properties of the CMs are investigated in the case of lossy metallic, dielectric, and dielectric–magnetic objects. For lossy conducting structures, both the radiated power and active power-based SIE formulations are considered. In the other cases, symmetric and nonsymmetric forms of the SIE- and VIE-based radiated power approaches are analyzed.

As was already pointed out in [5] and [10], the active power-based formulation does not provide modes with orthogonal far fields if losses are involved. Furthermore, [5] also argued that radiation power-based formulation would provide orthogonal far fields despite the complex symmetry of the operators. In this article, we have shown that this is not true in general. The far fields are orthogonal only if the geometry is sufficiently symmetric, such as a sphere, and the symmetry of the formulation has no effect on the far-field orthogonality. The main consequences of this result are as follows.

1) In the lossy case, the modes do not conform to the currently used definition of CMs providing a radiated-power orthogonal set of functions.
2) The power quantities associated with the modes of lossy structures cannot be treated independently, that is, the power computed from the sum of modal currents does not agree with the sum of modal powers.

The first property states that the CMs (based on the radiated power formulation) have different properties on the lossless and lossy cases:

1) In both cases, the far-field orthogonality is satisfied with respect to the symmetric product, but only in the lossless case this agrees with physical radiated power orthogonality.
2) In the lossless case, the eigenvalues are real, giving the ratio of reactive and radiated power. In the lossy case, they are complex, the real part having the same interpretation as in the lossless case and the imaginary part giving the ratio of dissipated and radiated power.

Since the non-orthogonality of the CMs is rather moderate with low losses, the modes can still give important physical insights into radiation properties and loss mechanisms of the structure [22].

Appendix

In this appendix, we give the definitions of the used volume and surface integral operators and currents.

A. Volume Integral Operators

For the VIE-based formulations, we define the following VIOs:

$$\mathcal{V}[\boldsymbol{f}](\boldsymbol{r}) = \left(\nabla\nabla\cdot + k_0^2\right)\int_V G_0(\boldsymbol{r},\boldsymbol{r}')\boldsymbol{f}(\boldsymbol{r}')\,dV' \quad (52)$$

$$\mathcal{U}[\boldsymbol{f}](\boldsymbol{r}) = \nabla\times\int_V G_0(\boldsymbol{r},\boldsymbol{r}')\boldsymbol{f}(\boldsymbol{r}')\,dV'. \quad (53)$$

Here, V is the volume of the object and G_0 is the scalar Green's function in free space with wavenumber k_0. The equivalent electric and magnetic volume currents are defined as

$$\boldsymbol{J}_V = -i\omega\varepsilon_0(\varepsilon_r - 1)\boldsymbol{E}, \quad \boldsymbol{M}_V = -i\omega\mu_0(\mu_r - 1)\boldsymbol{H}. \quad (54)$$

B. Surface Integral Operators

For the SIE-based formulations, we use SIOs

$$\mathcal{T}_j[\boldsymbol{f}](\boldsymbol{r}) = \frac{i}{k_j}\gamma_t\nabla\int_S G_j(\boldsymbol{r},\boldsymbol{r}')\nabla_s'\cdot\boldsymbol{f}(\boldsymbol{r}')dS' + i\,k_j\gamma_t\int_S G_j(\boldsymbol{r},\boldsymbol{r}')\boldsymbol{f}(\boldsymbol{r})dS' \quad (55)$$

$$\mathcal{K}_j^{\pm}[\boldsymbol{f}](\boldsymbol{r}) = \gamma_t\nabla\times\int_S G_j(\boldsymbol{r},\boldsymbol{r}')\boldsymbol{f}(\boldsymbol{r}')dS' \pm \frac{1}{2}\boldsymbol{n}(\boldsymbol{r})\times\boldsymbol{f}(\boldsymbol{r}). \quad (56)$$

Here, S is the surface of the object, $\boldsymbol{n}$ is the unit normal vector, k_j and G_j are the wavenumber and Green's function in domain j, $j = \{0, 1\}$, $\nabla_s\cdot$ is the surface divergence, and $\gamma_t\boldsymbol{f} = -\boldsymbol{n}\times(\boldsymbol{n}\times\boldsymbol{f})|_S$ is the tangential component on the surface S. The equivalent electric and magnetic surface currents are

$$\boldsymbol{J}_S = \boldsymbol{n}\times\boldsymbol{H} \quad \text{and} \quad \boldsymbol{M}_S = -\boldsymbol{n}\times\boldsymbol{E}. \quad (57)$$

References

[1] R. J. Garbacz, "Modal expansions for resonance scattering phenomena," *Proc. IEEE*, vol. 53, no. 8, pp. 856–864, Aug. 1965.
[2] R. J. Garbacz, "A generalized expansion for radiated and scattered fields," Ph.D. Dissertation, Dept. Elect. Eng., Ohio State Univ., Columbus, OH, USA, 1968.
[3] R. J. Garbacz and R. Turpin, "A generalized expansion for radiated and scattered fields," *IEEE Trans. Antennas Propag.*, vol. AP-19, no. 3, pp. 348–358, May 1971.
[4] R. Harrington and J. Mautz, "Theory of characteristic modes for conducting bodies," *IEEE Trans. Antennas Propag.*, vol. AP-19, no. 5, pp. 622–628, Sep. 1971.

[5] R. F. Harrington, J. R. Mautz, and Y. Chang, "Characteristic modes for dielectric and magnetic bodies," *IEEE Trans. Antennas Propag.*, vol. AP-20, no. 2, pp. 194–198, Mar. 1972.
[6] Y. Chang and R. F. Harrington, "A surface formulation for characteristic modes of material bodies," *IEEE Trans. Antennas Propag.*, vol. AP-25, no. 6, pp. 789–795, Nov. 1977.
[7] H. Alroughani, J. L. T. Ethier, and D. A. McNamara, "Observations on computational outcomes for the characteristic modes of dielectric objects," in *Proc. IEEE Antennas Propag. Soc. Int. Symp.*, Memphis, TN, USA, Jul. 2014, pp. 844–845.
[8] Z. T. Miers and B. K. Lau, "Computational analysis and verifications of characteristic modes in real materials," *IEEE Trans. Antennas Propag.*, vol. 64, no. 7, pp. 2595–2607, Jul. 2016.
[9] P. Yla-Oijala and H. Wallen, "PMCHWT-based characteristic mode formulations for material bodies," *IEEE Trans. Antennas Propag.*, vol. 68, no. 3, pp. 2158–2165, Mar. 2020.
[10] R. F. Harrington and J. R. Mautz, "Control of radar scattering by reactive loading," *IEEE Trans. Antennas Propag.*, vol. AP-20, no. 4, pp. 446–454, Jul. 1972.
[11] P. Ylä-Oijala, J. Lappalainen, and S. Järvenpää, "Characteristic mode equations for impedance surfaces," *IEEE Trans. Antennas Propag.*, vol. 66, no. 1, pp. 187–192, Jan. 2018.
[12] P. Ylä-Oijala, "Generalized theory of characteristic modes," *IEEE Trans. Antennas Propag.*, vol. 67, no. 6, pp. 3915–3923, Jun. 2019.
[13] P. Yla-Oijala, A. Lehtovuori, H. Wallen, and V. Viikari, "Coupling of characteristic modes on PEC and lossy dielectric structures," *IEEE Trans. Antennas Propag.*, vol. 67, no. 4, pp. 2565–2573, Apr. 2019.
[14] X.-Y. Guo, R.-Z. Lian, H.-L. Zhang, C.-H. Chan, and M.-Y. Xia, "Characteristic mode formulations for penetrable objects based on separation of dissipation power and use of single surface integral equation," *IEEE Trans. Antennas Propag.*, vol. 69, no. 3, pp. 1535–1544, Mar. 2021.
[15] P. Ylä-Oijala and H. Wallén, "Theory of characteristic modes for nonsymmetric surface integral operators, *IEEE Trans. Antennas Propag.*, vol. 69, no. 3, pp. 1505–1512, Mar. 2021.
[16] R. A. Horn and C. R. Johnson, *Matrix Analysis*. Cambridge, U.K.: Cambridge Univ. Press, 1990.
[17] Q. I. Dai, Q. S. Liu, H. U. I. Gan, and W. C. Chew, "Combined field integral equation-based theory of characteristic mode," *IEEE Trans. Antennas Propag.*, vol. 63, no. 9, pp. 3973–3981, Sep. 2015.
[18] P. Ylä-Oijala, H. Wallén, and S. Järvenpää, "Theory of characteristic modes for lossy structures: Formulation and interpretation of eigenvalues," *Int. J. Numer. Model., Electron. Netw., Devices Fields*, vol. 33, no. 2, pp. 1–18, Jun. 2019.
[19] M. T. H. Reid and S. G. Johnson, "Efficient computation of power, force, and torque in BEM scattering calculations," *IEEE Trans. Antennas Propag.*, vol. 63, no. 8, pp. 3588–3598, Aug. 2015.
[20] Y. Chen and C. F. Wang, *Characteristic Modes—Theory and Applications in Antenna Engineering*. Hoboken, NJ, USA: Wiley, 2015.
[21] C. Ehrenborg and M. Gustafsson, "Physical bounds and radiation modes for MIMO antennas," *IEEE Trans. Antennas Propag.*, vol. 68, no. 6., pp. 4302–4311, Jun. 2020.
[22] R. Luomaniemi, P. Yla-Oijala, A. Lehtovuori, and V. Viikari, "Designing hand-immune handset antennas with adaptive excitation and characteristic modes," *IEEE Trans. Antennas Propag.*, vol. 69, no. 7, pp. 3829–3839, Jul. 2021.

Matti Kuosmanen was born in Iisalmi, Finland, in 1996. He received the B.Sc. (Tech.) and M.Sc. (Tech.) degrees in electrical engineering from Aalto University, Espoo, Finland, in 2019 and 2021, respectively. He is currently pursuing the D.Sc. (Tech.) degree with Saab Finland Oy, Helsinki, Finland.

He has been with the Department of Electronics and Nanoengineering, School of Electrical Engineering, Aalto University, since 2020. His current research interests include wideband, beam steerable antenna arrays, and characteristic mode analysis.

Pasi Ylä-Oijala received the M.Sc. and Ph.D. degrees in applied mathematics from the University of Helsinki, Helsinki, Finland, in 1992 and 1999, respectively.

From 2004 to 2010, he was pointed as an Academy Research Fellow with the Academy of Finland, Helsinki. He is currently a Staff Scientist with the Department of Electronics and Nanoengineering, Aalto University, Espoo, Finland. His research interests include stable and efficient integral equation-based methods in computational electromagnetics, theory and application of characteristic modes, and electromagnetic modeling of complex material structures.

Jari Holopainen received the M.Sc. degree from the Helsinki University of Technology, Espoo, Finland, in 2005, the D.Sc. degree in electrical engineering from Aalto University, Espoo, in 2011, and the teacher's pedagogic qualification from the Häme University of Applied Sciences, Hämeenlinna, Finland, in 2015.

He is currently a University Lecturer with the Department of Electronics and Nanoengineering, School of Electrical Engineering, Aalto University. His current research interests include antennas and RF-powered devices.

Ville Viikari (Senior Member, IEEE) received the M.Sc. (Tech.) and D.Sc. (Tech.) (Hons.) degrees in electrical engineering from the Helsinki University of Technology (TKK), Espoo, Finland, in 2004 and 2007, respectively.

From 2001 to 2007, he was with the Radio Laboratory, TKK (now part of Aalto University, Espoo), where he studied antenna measurement techniques at submillimeter wavelengths and antenna pattern correction techniques. From 2007 to 2012, he was a Research Scientist and a Senior Scientist with the VTT Technical Research Centre, Espoo, where his research interests include wireless sensors, RFID, radar applications, MEMS, and microwave sensors. He was appointed as an Assistant Professor with Aalto University in 2012. He is currently a Professor and the Deputy Head of Department with the School of Electrical Engineering, Aalto University. He has authored or coauthored about 85 journal articles and 90 conference papers. He is an inventor in 16 granted patents. His current research interests include antennas for mobile devices and networks, antenna clusters and coupled arrays, RF-powered devices, and antenna measurement techniques.

Dr. Viikari is also a regional delegate of EurAAP. He was a recipient of the Young Researcher Award of the year 2014, presented by the Finnish Foundation for Technology Promotion and the IEEE Sensors Council 2010 Early Career Gold Award.